coatings

MDPI

Article

Chitosan-Based Coatings to Prevent the Decay of *Populus* spp. Wood Caused by *Trametes Versicolor*

Iosody Silva-Castro [1], Milagros Casados-Sanz [2], Agustín L. Alonso-Cortés [3], Pablo Martín-Ramos [4], Jesús Martín-Gil [1] and Luis Acuña-Rello [2,*]

1 Environmental Technology Laboratory, Department of Agricultural and Forestry Engineering, University of Valladolid, Avda. de Madrid 44, 34004 Palencia, Spain; iosody.silva@alumnos.uva.es (I.S.-C.); mgil@iaf.uva.es (J.M.-G.)
2 Wood Technology Laboratory, Department of Agricultural and Forestry Engineering, University of Valladolid, Avda. de Madrid 44, 34004 Palencia, Spain; milac@iaf.uva.es
3 Biotechnology Laboratory, Department of Agricultural and Forestry Engineering, University of Valladolid, Avda. de Madrid 44, 34004 Palencia, Spain; aleon@iaf.uva.es
4 Department of Agricultural and Environmental Sciences, EPS, Instituto Universitario de Investigación en Ciencias Ambientales de Aragón (IUCA), Universidad de Zaragoza, Carretera de Cuarte s/n, 22071 Huesca, Spain; pmr@unizar.es
* Correspondence: maderas@uva.es; Tel./Fax: +34-979-108397

Received: 23 October 2018; Accepted: 19 November 2018; Published: 22 November 2018

Abstract: Chitosan and chitosan oligomers are receiving increasing attention due to their antimicrobial properties. In the present study, they were assayed as a preventive treatment against white-rot decay of *Populus* wood (very important in economic and environmental terms), caused by *Trametes versicolor* fungus. Their capacity to incorporate different chemical species into the polymer structure with a view to improving their anti-fungal activity was also assessed by mixing oligo-chitosan with propolis and silver nanoparticles. The minimum inhibitory concentration of medium-molecular weight chitosan (MMWC), chitosan oligomers (CO), propolis (P), nanosilver (nAg), and their binary and ternary composites against *T. versicolor* was determined in vitro. Although all products exhibited anti-fungal properties, composites showed an enhanced effect as compared to the individual products: 100% mycelial growth inhibition was attained for concentrations of 2.0 and 0.2 mg·mL^{-1} for the CO-P binary mixture, respectively; and 2 µg·mL^{-1} for nAg in the ternary mixture. Subsequently, MMWC, CO, CO-P and CO-P-nAg composites were tested on poplar wood blocks as surface protectors. Wood decay caused by the fungus was monitored by microscopy and vibrational spectroscopy, evidencing the limitations of the CO-based coatings in comparison with MMWC, which has a higher viscosity and better adhesion properties. The usage of MMWC holds promise for poplar wood protection, with potential industrial applications.

Keywords: chitosan composites; FTIR; natural protectors; poplar wood; white-rot fungus

1. Introduction

In the field of wood protection, significant efforts have been devoted over the last decades to the assessment of natural products that can pose an alternative to other traditionally used chemical compounds, which have toxic effects on human beings and the environment [1]. In this sense, renewable polymers have attracted intense industrial interest, and, amongst them, chitosan has particularly promising application perspectives [2]. This natural polysaccharide derived from chitin is the second most abundant polymer in nature. Chitosan consists of chains of *N*-acetyl-D-glucosamine and D-glucosamine, and features a cationic character, which confers unique properties on it [3]. Among

its main characteristics, such as its bioactivity, non-toxicity or biodegradability, its antimicrobial effect is especially relevant [4–6]. Its activity against different fungi, gram positive and gram negative bacteria, is ascribed to the positive charge of amino group (NH_3^+), which interacts electrostatically with the surface of the cellular membrane, destabilizing it. As a consequence, the presence of chitosan inside the cell can lead to intracellular responses such as inactivation or blocking of enzymes activities, and of DNA transcription and translation [7,8].

The antifungal activity of chitosan not only depends on the fungus species, but also on its molecular weight (MW), polymerization degree (PD) or deacetylation degree (DD). For instance, chito-oligosaccharides with low MW, PD and DD have been reported to be more effective on phytopathogenic fungi than chitosan with higher MW, PD or DD [9–11].

Another known advantage from chitosan and its oligomers is associated with their sorption and chelating properties. The cationic nature of the polymer allows it to bind to different chemicals species, ranging from organic macromolecules to metal nanoparticles [12–14]. Natural oils or extracts of natural products can be incorporated into the chitosan matrix, for example, by cross-linking, producing solutions, films or beads [15–17]. In the particular case of propolis, its polyphenols have been reported to form hydrogen bonds and covalent bonds with the functional groups in chitosan [18]. This results in a stabilization of the propolis components in the polymer and in an enhancement of the antimicrobial activity due to a synergistic behaviour [19,20]. In the case of nanometals, for example, silver nanoparticles, chitosan and its derivatives can also be used in their synthesis, provided that chitosan can act as reducer as well as a stabilizer: the polymer matrix facilitates the nanoparticles preparation in one-step process, resulting in nanosilver with an ideal particle size [21]. Further, the resulting chitosan-nanosilver composites present a higher antimicrobial effect [22].

Chitosan-based composites have been successfully applied to the preservation of wood against mould fungi, as well as brown-rot and white-rot fungi [23–26], both in vitro and over beech and fir [27], Monterrey pine [28], Scot pine [29] and other hardwood and softwood species. Nonetheless, to the best of the authors' knowledge, to date no studies have focused on chitosan applications in order to protect poplar species. *Populus* spp., belonging to the Salicaceae family, are one of the most cultivated woody plants for industrial purposes. Its wood is one of the least expensive hardwoods and, although rarely used in the production of fine furniture, it is extensively used for pulp, panel productions and many other commercial applications [30,31]. These fast-growing trees therefore have a large economic impact worldwide, together with a significant importance from an environmental perspective [32]. According to EN 350:2016 rule, poplar wood is a non-durable species [33], and some studies have evidenced that it is highly susceptible to *Trametes versicolor* [34,35]. Therefore, chitosan-based composites can be applied as a potential tool to avoid the white-rot decay of *Populus* spp. wood, improving its natural durability and increasing its technological uses.

The first objective of the study was to investigate the in vitro antifungal activity against *T. versicolor* of two different molecular weight chitosan treatments: medium molecular weight chitosan (MMWC) and chitosan oligomers (CO); the latter—which resulted in a better minimum inhibitory concentration (MIC) value—was also tested in binary and ternary combinations with propolis (P) and nanosilver (nAg). In a second stage, once the MIC values had been determined, the best treatments were evaluated on poplar wood blocks as surface protectors to prevent wood decay, with a view to their practical application. Wood biodegradation was monitored by microscopy and by tracking chemical alterations. For this latter purpose, Fourier-transform infrared spectroscopy (FTIR) technique was chosen, provided that it is quickly consolidating as an easy-technique to characterize and evaluate the decay of wood [36–38].

2. Materials and Methods

2.1. Reagents, Fungal Isolate and Wood

Medium molecular weight chitosan (CAS No. 9012-76-4), with 60–130 kDa and 90% deacetylation, was acquired from Hangzhou Simit Chemical Technology Co. (Hangzhou, China). Propolis, with a content of ca. 10% w/v of polyphenols and flavonoids, came from the Duero river basin region (Burgos, Spain). Silver nitrate (CAS number 7761-88-8) was supplied by Merck Millipore (Darmstadt, Germany). All the other reagents used to synthetize or prepare the solutions were of analytical grade.

The isolate of *T. versicolor* (L.) Lloyd 1920 (DSM 3086 strain, CECT 20804) was supplied by the Spanish Type Culture Collection (Valencia, Spain) and was cultivated on potato dextrose agar (PDA) (supplied by Scharlau, Barcelona, Spain) for all assays.

The wood blocks were supplied by the Wood Technology Laboratory at Universidad de Valladolid from *P. euroamericana* I-214 clone.

2.2. Chitosan-Based Solutions

The solutions of MMWC, CO, P, nAg and the CO-based binary and ternary mixtures—tested in vitro for the inhibition of *T. versicolor* mycelial growth and as wood coatings—were prepared starting from commercial medium MW chitosan, which was dissolved in acetic acid (1%) under constant stirring at 60 °C for 2 h. The pH value was then adjusted from 4.5 to 6.5 with potassium methoxide. Subsequently, oligo-chitosan was prepared by oxidative degradation of the solubilized MMWC by addition of hydrogen peroxide (0.3 M), obtaining a MW of 2 kDa [39]. Propolis constituents soluble in ethanol were extracted by grinding the resin and adding it to a hydroalcoholic solution (ethanol 30%), followed by stirring for 72 h at room temperature, and by filtration with a stainless steel 220 mesh to remove insoluble particles [40]. Silver nanoparticles were synthetized by a sonication method: 50 mL of silver nitrate (50 mM) were first mixed with 50 mL of sodium citrate (30 mM) as a reducing agent, and the solution was heated up to 90 °C until it turned from colourless to pale yellow, which then became more intense. The yellowish solution was sonicated for 3–5 min and allowed to stabilize for at least 24 h in a refrigerator at 5 °C [41].

The binary and ternary solutions were prepared according to Martín-Gil et al. [42], by mixing of the solutions described above at the desired concentrations (Table 1), followed by sonication for 1 min with a probe-type UIP1000hdT ultrasonicator (Hielscher, Teltow, Germany; 1000 W, 20 kHz).

Table 1. Concentrations used in the in vitro experiments (medium molecular weight chitosan (MMWC), COs and P are given in mg·mL^{-1}, and that of nAg in µg·mL^{-1}).

Treatment	Concentration				
Control			0.0		
MMWC	1.0	2.0	4.0	7.0	10.0
CO	1.0	1.5	2.0	2.5	3.0
P	0.1	0.2	0.3	0.4	0.5
nAg	1.0	1.5	2.0	2.5	3.0
CO-P	0.5–0.05		1.0–0.1		2.0–0.2
CO-nAg	0.5–0.5		1.0–1.0		2.0–2.0
P-nAg	0.05–0.5		0.1–1.0		0.2–2.0
CO-P-nAg	0.5–0.05–0.5		1.0–0.1–1.0		2.0–0.2–2.0

2.3. In Vitro Assays

Each solution was incorporated into PDA at a ratio of 1:10 (*v/v*). PDA had been sterilized for 20 min at 121 °C and had been cooled down to 50 °C before the addition of the treatments (or of distilled and sterilized water in the case of control). 20 mL of the medium were then spread in Petri dishes and, once they had solidified, 5 mm in diameter discs of young mycelia of *T. versicolor* were placed on the center of each Petri dish, followed by incubation in the dark at 25 °C and 65% HR. Three

replicates were performed for each treatment. Finally, radial growth was measured on a daily basis until the mycelium reached the edges of the control Petri dish (8 days), and the inhibition growth percentage was calculated.

2.4. Wood Coating Assays

On the basis of the in vitro study results, the best treatments (either individual, binary or ternary mixtures) were assayed as a coating over poplar wood in order to prevent its degradation against *T. versicolor* fungus.

Small poplar wood blocks ($5 \times 5 \times 20$ mm^3), previously dried at 103 ± 2 °C to determinate their initial dry weight, were soaked in the different solutions: water (control), MMWC, CO, CO-P and CO-P-nAg (36 blocks per treatment) for 12 h at room temperature. A concentration of 20 mg·mL^{-1} for MMWC, 20 mg·mL^{-1} for CO, 2 mg·mL^{-1} for P, and 20 µg·mL^{-1} for nAg were used. These doses, which were ten times higher than the obtained MIC values from binary and ternary mixtures, were chosen on the basis of adsorption, penetration and fixation tests, so as to compensate for the influence of the dipping time on the uptake of the preservative solution and to minimize wood swelling, as reported by Eikenes et al. [29] and Larnoy et al. [43]. Excess of liquid was then removed and the wood blocks were dried in a chamber for 24 h at 45 °C. The coated blocks were placed on Petri dishes—six per plate—newly covered until the edges by *T. versicolor* mycelia, which were again incubated at 27 °C and 70% of relative humidity (RH) for 30 days.

One Petri dish, with six blocks, of each treatment was removed every 5 days for analysis. The mycelia on the wood surface were carefully cleaned, the small blocks were then dried at 103 ± 2 °C to quantify their dry weight after fungal attack, and the mass loss was determined by subtracting it from the initial weight according to EN 113:1996 [44].

2.5. Microscopy and FTIR Studies

In order to monitor wood degradation, a Leica (Wetzlar, Germany) microtome was used to cut thin wood sections (30 µm), which were analyzed by optical microscopy (with a Leica DMLM Transmission Optical Microscope). Thin cut sections were also grinded and mixed with KBr (in 1:300 ratio) to prepare pellets to study the FTIR spectrum by direct transmittance technique, using a Thermo Scientific (Waltham, MA, USA) Nicolet iS50 FTIR spectrometer. The spectra were collected in the 400–4000 cm^{-1} region at room temperature with a 1 cm^{-1} spectral resolution; a total of 64 scans were co-added and the resulting interferogram was averaged. The obtained spectra were corrected using the advanced ATR correction algorithm available in OMNIC software suite (Thermo Scientific, Waltham, MA, USA), and were normalize using the 1048 cm^{-1} band, assigned to CO stretching, in agreement with Colom et al. [36].

2.6. Statistical Analyses

All the statistical analyses were performed using R software (v. 3.4.4) (R Development Core Team, 2018). A total of 216 data, corresponding to 15 different individual groups (6 samples × 3 preservative agents × 5 concentration levels), 1 control group (6 samples), 3 binary groups (6 samples × 3 groups × 3 concentration levels) and 1 ternary group (6 samples × 3 levels) were analysed. Prior to the analyses, the assumptions of independence, normality and homoscedasticity were checked for all groups. Since the data structure did not meet the normality requirement, checked with Shapiro-Wilks test, or the homoscedasticity requirement, checked with Bartlett's test, the usual comparative analysis (ANOVA) could not be used. Bootstrapping, Welch's test and robust homogenous groups were used instead.

3. Results and Discussion

3.1. Minimum Inhibitory Concentration

The antifungal activity of the chitosan-based composites against *T. versicolor* was evaluated in a typical in vitro inhibition growth experiment. The results, collected after seven days of incubation, are shown in Table 2. MMWC presented a moderate activity against mycelial growth, with significant differences in comparison with the control treatment. However, low doses resulted in a low inhibition and higher concentrations (up to 10 mg·mL^{-1}) were needed to approach 100% mycelial growth inhibition. In contrast, CO exhibited a high inhibitory activity even at the lowest doses; for example, 1 mg·mL^{-1} of CO inhibited 79% of mycelial growth. As expected, the increase in CO concentration resulted in an increase of *T. versicolor* mycelial growth inhibition, attaining 100% inhibition (MIC) at a concentration of 3 mg·mL^{-1}.

Table 2. Effect of treatment concentration on the mycelial growth of *T. versicolor* (in vitro) seven days after incubation. The concentrations of MMWC, COs and P are given in mg·mL^{-1}, and that of nAg in μg·mL^{-1}.

Treatment	Concentration	Inhibition Percentage (%) Mean-Confidence Interval and Homogeneous Groups		Shapiro Wilk *p*-Value	Levene's Test *p*-Value	Welch's Test *p*-Value
Control	0.0	0.000 ± 0.000	C	0.000	–	–
MMWC	1.0	22.708 ± 2.027	a	0.324	0.08629	0.0000
	2.0	42.083 ± 1.429	b	0.505		
	4.0	75.375 ± 1.970	e	0.377		
	7.0	90.250 ± 1.846	i	0.988		
	10.0	95.542 ± 1.331	j k	0.001		
CO	1.0	78.750 ± 1.094	f	0.110	0.0417	0.0000
	1.5	87.708 ± 0.857	h	0.035		
	2.0	92.333 ± 0.991	i j	0.433		
	2.5	97.000 ± 0.992	k	0.680		
	3.0	99.997 ± 0.004	l	0.001		
P	0.1	84.541 ± 1.135	g	0.836	0.0207	0.0000
	0.2	88.333 ± 1.173	i	0.911		
	0.3	93.333 ± 1.148	j	0.850		
	0.4	97.500 ± 0.909	k	0.421		
	0.5	99.997 ± 0.004	l	0.001		
nAg	1.0	85.000 ± 1.270	g	0.960	0.0214	0.0000
	1.5	91.333 ± 1.221	h	0.843		
	2.0	94.217 ± 1.177	j	0.473		
	2.5	97.333 ± 0.753	k	0.725		
	3.0	99.997 ± 0.004	l	0.001		
CO-P	0.5–0.05	51.458 ± 2.472	c	0.540	0.0037	0.0000
	1.0–0.1	89.167 ± 0.451	h	0.001		
	2.0–0.2	99.997 ± 0.003	l	0.001		
CO-nAg	0.5–0.5	64.583 ± 0.427	d	0.001	0.0281	0.0000
	1.0–1.0	84.583 ± 0.740	g	0.091		
	2.0–2.0	99.996 ± 0.003	l	0.001		
P-nAg	0.05–0.5	47.292 ± 1.673	c	0.212	0.1652	0.0000
	0.1–1.0	84.167 ± 0.639	g	0.001		
	0.2–2.0	99.997 ± 0.004	l	0.001		
CO-P-nAg	0.5–0.05–0.5	77.500 ± 1.081	f	0.110	0.0190	0.0000
	1.0–0.1–1.0	85.208 ± 1.348	g	0.804		
	2.0–0.2–2.0	99.997 ± 0.004	l	0.001		

As regards the differences observed between the activities of MMWC and CO, the results obtained in this study would agree with other in vitro assays reported in the literature, such as those mentioned in the introduction or those by Matei et al. [41] and Rahman et al. [9], who found a better antifungal activity for low MW (less than 20 kDa) chitosan than for medium or high MW (more than 140 kDa)

chitosan. Nonetheless, it should be clarified that this behaviour may not be extrapolated to all fungi: for instance, Younes et al. [10] found that fungal growth decreased with increasing MW for *Fusarium oxysporum*, thus pointing at the need to evaluate the optimum MW for each species.

In relation to the MIC, Stössel and Leuba [45] reported that—for native chitosan—MIC values could vary from 0.001 to 2.5 mg·mL^{-1}, depending on the phytopathogenic fungus. According to Rabea et al. [46], the MIC value depends on factors such as the type of chitosan, the fungus under study, the chemical or nutrient composition of the substrate and the environmental conditions. Another work on *Sphaeropsis sapinea* and *Trichoderma harzianum* wood-degrading fungi suggested that the application of 1 mg·mL^{-1} of low-molecular weight chitosan reduced growth rate by a factor of 3 with respect to the control [47], in line with the results reported by Silva-Castro et al. [40], who found that 1 mg·mL^{-1} of CO inhibited 86% of the mycelial growth of *Heterobasidium annosum* basidiomycete fungus. Thus, in view of aforementioned MIC values, it may be inferred that *T. versicolor* would show an intermediate sensitivity (i.e., would be moderately sensitive) to chitosan/CO alone, albeit such resistance would not be as high as that of, for example, *Macrophomina phaseolina* (for which MIC values of water-soluble chitosan as high as 12.5 mg·mL^{-1} were found [48]). Consequently, it seemed necessary to explore binary or ternary combinations with other compounds with antifungal activity in order to search for synergies and to attain lower MIC values.

Propolis exhibited a higher antifungal activity against *T. versicolor* than CO: in propolis-based treatments, 85% growth inhibition was attained with 0.1 mg·mL^{-1}, with a MIC value of 0.5 mg·mL^{-1} (six times lower than MIC of CO). The use of propolis as an antifungal agent is well-known, and its effectiveness has been proved against *Candida* spp. and other human pathogens [49–51]. This has promoted its use in the production of films to control foodborne fungi [52,53]. With regard to phytopathogenic oomycetes (*Phytophthora alni* and *Phytophthora plurivora*), 0.1 mg·mL^{-1} of propolis ethanolic extract resulted in 100% inhibition [40]. Although there is no data concerning propolis action against white-rot fungi (a thorough search of the relevant literature did not yield any reports on the antifungal activity of propolis ethanolic extracts to control *T. versicolor* growth), other natural products were assessed by Zhang et al. [54], who evaluated the activity against white-rot fungi of 41 monoterpenes (which are part of the composition of propolis). They found that carvacrol at a concentration of 0.4 mg·mL^{-1} led to 100% growth inhibition against *Trametes hirsuta*, *Schizphylhls commune*, and *Pycnoporus sanguineus*, that is, its MIC value was similar to that reported herein for P.

Regarding nAg treatments, just 1 µg·mL^{-1} led to 85% mycelial growth inhibition, which increased up to 100% at a concentration of 3 µg·mL^{-1} (MIC value). It should be clarified that the remarkable ability of nanosilver to inhibit fungal growth depends not only on the fungal species, but on the nanoparticles characteristics—shape, size, synthesis method, stabilization, and so forth [55], which makes direct comparisons difficult. For instance, a study was carried out to test three types of nanosilver against eighteen plant pathogenic fungi, and while no variation was detected at relatively low doses (10 µg·mL^{-1}), at higher concentrations (100 µg·mL^{-1}) the maximum inhibition for most fungi was shown by dark brown colloid nanoparticles [56]. Apropos of wood-degrading fungi, silver nanoparticles synthesized using turnip leaf extract were assayed against four fungi, showing slight to moderate growth inhibition (with 2 and 4 mg of nanosilver on paper discs) [57]. Although in both studies the nanoparticles presented a reasonably good activity, the MIC value found in the present study indicates that *T. versicolor* would be very sensitive to nAg.

Since the antifungal activity of CO was noticeably higher than that of MMWC, only composites of CO, P and nAg, in binary and ternary mixtures, were assessed. These composites presented significant differences in comparison with the same concentrations of individual products. The CO-P binary composites inhibited 100% of mycelial growth with 2 and 0.2 mg·mL^{-1}, respectively (vs. MIC values of 3 mg·mL^{-1} and 0.5 mg·mL^{-1} for individual treatments with CO and P, respectively), suggesting that the mixture of both natural products would enhance the antifungal activity against *T. versicolor*. A similar behaviour has also been reported by other authors, who observed that the addition of propolis

to chitosan films enhanced their in vitro antimicrobial effect [18]. However, it is worth noting that this synergistic behaviour cannot be extrapolated to all pathogens, provided that Mascheroni et al. [58] reported disparate results for different foodborne fungi, with lower MICs for propolis-only treatments than for chitosan-propolis beads in some cases. Likewise, Silva-Castro et al. [40] found no statistically significant differences between CO-P composites and propolis-only treatments against *P. alni* and *P. plurivora*.

Apropos of the binary CO-nAg composite, it resulted in 100% growth inhibition (MIC value) for a concentration of 2 mg·mL^{-1} and 2 µg·mL^{-1}, respectively (lower than the MICs of the corresponding individual products too). However, a different behaviour was observed at lower doses of the mixture, provided that significant differences between CO-nAg and nAg-only treatments were not found at 0.1 µg·mL^{-1}, suggesting that the nAg dose in the composite would be crucial (as noted above, *T. versicolor* showed a much higher sensitivity to nAg than to chitosan). The results at a higher concentration would be in good agreement with other studies in which it has been demonstrated that the composites of both products have a greater antifungal activity [59], while the behaviour found at lower nAg doses would be in line with the findings of Velmurugan et al. [60], who reported that chitosan with silver nanosized particles exhibited a similar antifungal effect than the nanoparticles alone against wood staining fungi, given the remarkable antifungal activity of the latter.

The third binary mixture, P-nAg, presented a MIC value of 0.2 mg·mL^{-1} and 2 µg·mL^{-1} for P and nAg, respectively, which was also lower than MICs found for the treatments based on the individual products. However, at lower concentrations (0.1 mg·mL^{-1} and 0.1 µg·mL^{-1}) of P-nAg, again there were not significant differences in comparison with the nAg individual solutions, resulting in similar inhibition percentages (around 85%). This would reinforce the interpretation discussed above, in which nAg would play a key role in *T. versicolor* inhibition, given the high sensitivity of the fungus to this component. The dependence of the behaviour on the particular pathogen is evidenced by the different results reported for the control of other forest pathogens: Silva-Castro et al. [40] found that P-nAg composites showed a similar effect to that of CO against *Fusarium circinatum*, a lower effect than that of CO against *Diplodia pinea*, and an enhanced behaviour versus CO-only treatments for the control of *Phytophthora cambivora*.

Finally, the ternary mixture reached full mycelial growth inhibition at a MIC value of 2 mg·mL^{-1} of CO, 0.2 mg·mL^{-1} of P and 0.2 µg mL^{-1} of nAg, so it would not present an advantageous behaviour as compared to the binary composites. This same CO-P-nAg ternary composite has been tested against *Diplodia seriata* [41], *Bipolaris oryzae* [61] and eight forest phytopathogenic fungi [40], attaining a higher inhibition than the individual or binary products at concentrations of 20–25 mg·mL^{-1}, but leading to a similar effect than that of binary solutions at lower concentrations, as it happens in the present study. Paradoxically, at the lowest dose assayed herein (0.5 mg·mL^{-1} of CO, 0.05 mg·mL^{-1} of P and 0.5 µg·mL^{-1} of nAg), CO-P-nAg showed a noticeable higher antifungal effect against *T. versicolor* (79% inhibition) than the binary mixtures (51%, 64% and 47% inhibition for CO-P, CO-nAg and P-nAg, respectively).

3.2. Wood Preservation Assays

3.2.1. Weight Loss

Surface treatments with the chitosan-based composites were applied to mini-blocks of poplar wood in order to prevent white-rot decay. Weight loss was recorded every 5 days (see Table 3). The non-treated mini-blocks (control) and those treated with chitosan oligomers-based treatments (CO, CO-P and CO-P-nAg) started losing weight from second sampling (10 days), in contrast with those treated with MMWC. In the third sampling (after 15 days), degradation caused by *T. versicolor* increased for all treatments, although with significant differences among the control and all the other treatments. Non-covered blocks exhibited a weight loss of up to 27.3%, followed by those treated with CO-P-nAg (22.8%), CO-P (14.7%), CO (7%) and MMWC (3%). The differences between coated and

non-coated samples further increased in the fourth sampling (after 20 days), in which the weight loss only increased slightly for the treated blocks, while degradation reached 32.9% for the control. 25 days after the exposure to fungus, the wood treated with MMWC still exhibited the lowest weight loss (7.7%), while weight loss for the CO-based treatments increased, albeit still with significant differences as compared to the control (39.8%). In the last sampling (after 30 days), the wood blocks treated with the ternary composite reached a similar degradation level to that of the control—without significant differences, in contrast with MMWC-treated samples, for which the weight loss (10.8%) remained well-below that of the control (42.3%).

Table 3. Effect of coating treatments and time on weight loss for *Populus* spp. wood-blocks exposed to white-rot fungus *T. versicolor*.

Treatment	Time (days)	Weight Loss (%) Mean-Confidence Interval and Homogeneous Groups		Shapiro Wilk *p*-Value	Levene's Test *p*-Value	Welch's Test *p*-Value
Control	5	0.138 ± 0.155	a	0.004	0.1973	0.0000
	10	5.352 ± 1.315	b c	0.079		
	15	27.261 ± 3.037	i j	0.127		
	20	32.888 ± 4.233	j k	0.073		
	25	39.774 ± 2.036	l	0.949		
	30	42.353 ± 1.866	l	0.470		
MMWC	5	0.000 ± 0.000	a	0.000	0.1132	0.0000
	10	0.000 ± 0.000	a	0.000		
	15	3.478 ± 0.541	b	0.534		
	20	7.177 ± 0.570	c	0.900		
	25	10.157 ± 1.095	d	0.955		
	30	11.455 ± 1.171	d	0.412		
CO	5	0.000 ± 0.000	a	0.000	0.0001	0.0000
	10	4.311 ± 0.883	b	0.825		
	15	6.570 ± 1.226	c	0.759		
	20	13.524 ± 0.937	e	0.999		
	25	22.190 ± 0.890	h	0.961		
	30	26.871 ± 1.164	i	0.373		
CO-P	5	0.000 ± 0.000	a	0.000	0.0254	0.0000
	10	7.567 ± 0.889	c	0.610		
	15	13.578 ± 1.084	e	0.996		
	20	17.276 ± 1.154	f	0.869		
	25	29.662 ± 1.174	j	0.340		
	30	32.856 ± 1.039	k	0.289		
CO-P-Ag	5	0.000 ± 0.000	a	0.000	0.0342	0.0000
	10	10.615 ± 1.071	d	0.138		
	15	20.150 ± 1.185	g	0.660		
	20	26.864 ± 1.154	i	0.971		
	25	35.074 ± 1.341	k	0.762		
	30	39.943 ± 2.357	l	0.882		

The poplar wood mini-blocks from the control treatment presented a higher degradation rate than those of beech wood exposed to *T. versicolor* in the study carried out by Mohebby [38]: in the latter, a weight loss of ca. 20% was recorded on the 28th day of the experiment, half of the one recorded in this study after 30 days (42%). This can be readily ascribed to the high susceptibility of *Populus* spp. wood to this fungus [32,34].

With regard to the differences in the weight loss rates for the treated samples, although most treatments resulted in a slower degradation than that of the control, MMWC was clearly the most effective protective agent (Figure 1). This should be ascribed to its higher viscosity and better adhesive properties, adhesion is directly related to the DD of chitosan: if chitosan DD increases, the number of positive charges also increases, which leads to improved adhesive properties [62], which would result in a better coating on the surface of wood blocks. This would agree with Eikenes et al. [29], who demonstrated that medium MW chitosan (at a concentration of 50 mg·mL^{-1}) was able to avoid the decay caused by brown-rot fungi on Scots pine, performing better than low MW chitosan, as

it also happened in this study. Low doses of this type of chitosan (lower than 10 mg·mL^{-1}) were also found to be effective against white-rot fungi, according to Nowrouzi et al. [27]. Of course, the wood preservation effect would largely depend on the concentration of chitosan, as demonstrated by El-gamal et al. [23] in relation to the growth of fungi on treated wood samples from historic artefacts (fungal growth decreased with the increase in chitosan concentration).

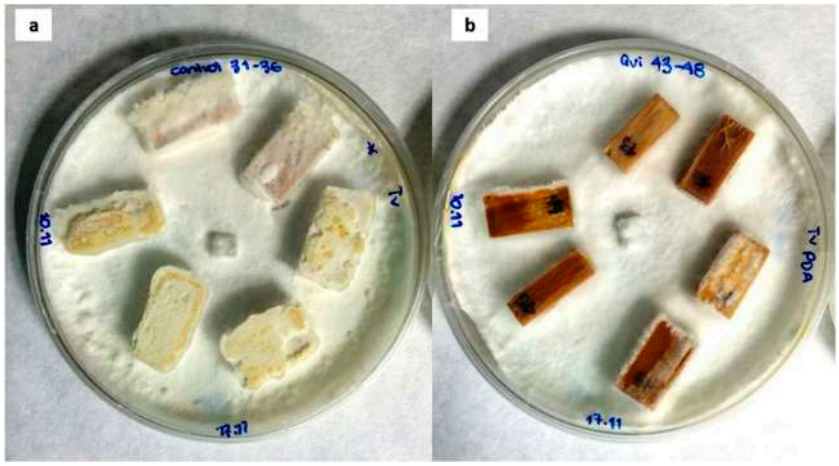

Figure 1. Poplar wood samples 30 days after exposure to *T. versicolor*: (**a**) control wood sample and (**b**) sample treated with medium molecular weight chitosan.

Concerning the effectiveness as wood protecting agents of the composites, it was lower than that of the chitosan-only treatments (especially in comparison with MMWC), in contrast with the results from the in vitro assays. This unexpected result may be explained by their low viscosity and poor adhesion properties [63], which may be enhanced by adding thickening agents to chitosan oligomers, such as natural gums, starches, pectins, alginate and carrageenan [64]; by preparing CO–clay based composite materials [65]; or by using other impregnation procedures (involving vacuum and pressure).

In view of aforementioned results, MMWC would be the preferred choice for industrial applications, not only due to its higher effectiveness, but also because of its fast and facile preparation process.

3.2.2. Wood Degradation Monitoring

The decay of the wood-blocks was tracked using microscopy techniques. In the control sample, changes such as cavities in the cell wall and a quick development of fungal hyphae were easily recognized, the change between undecayed control wood and the last sampling (after 30 days) can be observed by comparing Figure 2a,b, respectively. The hyphae progressively increased over the 30 days, resulting in a strong structure interconnected with the wood one, as well as in holes in the cell walls and in a general degradation of the vessels and fibres of the poplar wood, confirming the high susceptibility of *Populus* spp. wood to *T. versicolor* [32]. Analogous effects were identified with SEM microscopy on uncovered blocks of the softwood from *Paulownia fortune* attacked by *T. versicolor* [66], providing evidence that the fungus can tunnel along the cellulose microfibrils, resulting in the formation of holes in transverse sections. Changes in the samples impregnated with MMWC were much less evident, even 30 days after exposure, with an associated weigh loss of 10% (Figure 2c).

FTIR spectroscopy was also used to follow the decay—by tracking chemical changes—of the poplar wood mini-blocks. The infrared spectrum of undecayed control wood (Figure 3) was almost identical to that of *Fagus sylvatica* [37], featuring a broad band at around 3400 cm^{-1} (corresponding to a convolution of O–H and N–H stretching vibration bands, at 3480 and 3270 cm^{-1}, respectively) and a band at around 2997 cm^{-1} (C–H stretching), which was also observed in the control and MMWC-coated wood samples 30 days after the exposure to *T. versicolor*. In view of the very small

shifts observed in the first band for the MMWC coating, a low interaction of the solution with the wood may be inferred. When such interaction occurs, hydrogen bonds suffer a redistribution and the N–H band disappears [67].

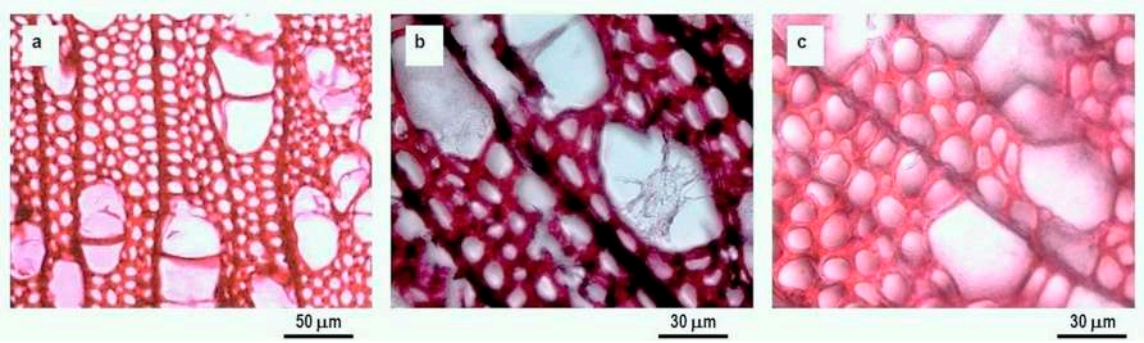

Figure 2. Optical micrographs (at 500× magnification) of the surface of poplar wood samples: (**a**) undecayed control wood sample prior to exposure to *T. versicolor*; (**b**) control wood sample 30 days after exposure to *T. versicolor*; and (**c**) sample treated with medium molecular weight chitosan 30 days after exposure to *T. versicolor*.

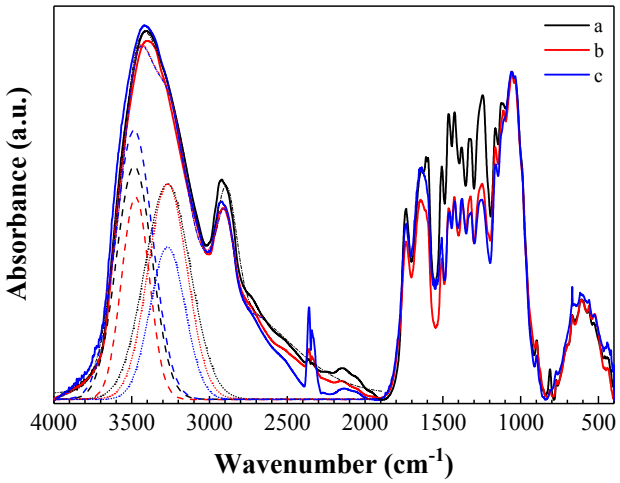

Figure 3. Normalized Fourier transform infrared (FTIR) spectra of poplar wood samples: (**a**) undecayed control wood sample prior to exposure to *T. versicolor*; (**b**) control 30 days after exposure to *T. versicolor*; and (**c**) sample treated with medium molecular weight chitosan 30 days after exposure to *T. versicolor*. A deconvolution of O–H (dashed lines) and N–H (dotted lines) bands, together with the cumulative peak fit (short dash-dot lines), is shown.

Many well-defined bands could also be observed in the fingerprint region, between 1800 and 600 cm^{-1}: at 1740 cm^{-1} (unconjugated C=O from xylans in hemicellulose and/or C–O carbonyl band); at 1650 cm^{-1} (conjugated C–O in aromatic ring and O–H in absorbed water); at 1606 cm^{-1} and 1510 cm^{-1} (C=C aromatic skeletal vibrations in lignin); at 1465 cm^{-1} (CH_3 asymmetric bending in lignin); at 1425 cm^{-1} (CH_2 bending in cellulose); at 1380 cm^{-1} (C–H deformation in cellulose and hemicellulose); at 1327 cm^{-1} (C–O in syringyl and guaiacyl rings and/or O–H in plane bending in cellulose); at 1247 cm^{-1} (syringyl ring and/or C–O stretching in lignin and xylan); at 1165 cm^{-1} (C–O–C symmetric stretching in cellulose); at 1117 cm^{-1} (aromatic skeletal and C–O stretching vibrations); at 1044 cm^{-1} (C–O stretching in cellulose and hemicellulose); and at 903 cm^{-1} (C–H out of phase ring stretching in cellulose) [36–38,68,69].

Upon comparison of the spectra of the undecayed control sample and the control block at the end of the experiment, a decrease in the intensity of the band at 1606 and 1510 cm^{-1}, associated with lignin, and an increase in the intensity of the band at 1650 cm^{-1} (conjugated C–O from aromatic ring of xylans

in hemicellulose) could be observed, suggesting a preference of the fungus for lignin [37]. In relation with the MMWC-treated wood blocks, only some slight changes in the chemical structure of the poplar wood were found, for example, a decrease in the intensity of carbonyl band at 1740 cm^{-1} (probably due to the opening of conjugated bonds and formation of new linkages with other groups in the hemicellulose), in good agreement with the study conducted by Nowrouzi et al. [27] on beech wood.

4. Conclusions

The effectiveness of chitosan and the chitosan-based composites as wood preservatives against white-rot fungus *T. versicolor* was assessed, both in vitro and as surface protection treatments. The minimum inhibitory concentration (MIC) against mycelial growth was determined for the individual components (MMWC, CO, P and nAg) and their binary (CO-P, CO-nAg, P-nAg) and ternary (CO-P-nAg) mixtures. A higher in vitro antifungal activity of CO versus MMWC was observed, as well as a better performance of the binary mixtures in comparison with the individual products (full mycelium growth inhibition was attained at concentrations of 2 $mg{\cdot}mL^{-1}$ for CO, 0.2 $mg{\cdot}mL^{-1}$ for P and 2 $\mu g{\cdot}mL^{-1}$ for nAg when any two of the products were combined). Nonetheless, no significant improvements associated with the ternary composite over its binary counterparts were found for this fungus. The protective effect of the composites as coatings of poplar wood blocks was then evaluated, monitoring the wood decay over a 30-day period after exposure to the fungus in terms of weight loss and by microscopy and vibrational spectroscopy techniques. MMWC was found to be best protective agent, probably due to its higher viscosity and adhesion properties. Although a remarkable potential of the all treatments was evidenced by the in vitro tests, the medium molecular weight chitosan was the best considering commercial applications.

Author Contributions: Conceptualization: I.S.-C., M.C.-S., A.L.A.-C., P.M.-R., J.M.-G. and L.A.-R.; Formal Analysis: L.A.-R., I.S.-C. and P.M.-R.; Investigation: I.S.-C., M.C.-S., A.L.A.-C., and J.M.-G.; Methodology: A.L.A.-C., L.A.-R. and J.M.-G.; Resources: M.C.-S., A.L.A.-C., L.A.-R. and J.M.-G.; Supervision: L.A.-R. and J.M.-G.; Validation: L.A.-R., I.S.-C., J.M.-G. and P.M.-R.; Visualization: P.M.-R.; Writing—Original Draft: I.S.-C.; Writing—review & editing, L.A.-R., I.S.-C., J.M.-G., M.C.-S., A.L.A.-C. and P.M.-R.

Funding: The APC was funded by Instituto Tecnológico Agrario y Agroalimentario (ITAGRA, Spain).

Acknowledgments: Authors would like to thank to Spanish Type Culture Collection (Valencia, Spain) for the fungus supply. I.S.-C. would like to gratefully acknowledge the financial support of the National Council for Science and Technology (CONACYT) of Mexico, through PhD Scholarship ref. no. 329975. P.M.-R. acknowledges Santander Universidades support through the "Becas Iberoamérica Jóvenes Profesores e Investigadores, España" scholarship programme.

Conflicts of Interest: The authors declare no conflict of interest. The founding sponsors had no role in the design of the study; in the collection, analyses, or interpretation of data; in the writing of the manuscript, and in the decision to publish the results.

References

1. Singh, T.; Singh, A.P. A review on natural products as wood protectant. *Wood Sci. Technol.* **2012**, *46*, 851–870. [CrossRef]
2. Thakur, V.K.; Thakur, M.K. Recent advance in graft copolymerization and application of chitosan: A review. *ACS Sustain. Chem. Eng* **2014**, *2*, 2637–2652. [CrossRef]
3. Kumar, M.N.R. A review of chitin and chitosan applications. *React. Funct. Polym.* **2000**, *46*, 1–27. [CrossRef]
4. Ngo, D.-H.; Vo, T.-S.; Ngo, D.-N.; Kang, K.-H.; Je, J.-Y.; Pham, H.N.-D.; Byun, H.-G.; Kim, S.-K. Biological effects of chitosan and its derivatives. *Food Hydrocoll.* **2015**, *51*, 200–216. [CrossRef]
5. Ma, Z.; Garrido-Maestu, A.; Jeong, K.C. Application, mode of action, and in vivo activity of chitosan and its micro- and nanoparticles as antimicrobial agents: A review. *Carbohydr. Polym.* **2017**, *176*, 257–265. [CrossRef] [PubMed]

6. Silva-Castro, I.; Martín-Ramos, P.; Matei, P.M.; Fernandes-Correa, M.; Hernánez-Navarro, S.; Martín-Gil, J. Eco-friendly nanocomposites of chitosan with natural extracts, antimicrobial agents, and nanometals. In *Handbook of Composites from Renewable Materials*; Thakur, V.K., Thakur, M.K., Kessler, M.R., Eds.; Scrivener Publishing LLC: Beverly, MA, USA, 2017; Volume 8, pp. 35–60.
7. Kumaraswamy, R.V.; Kumari, S.; Choudhary, R.C.; Pal, A.; Raliya, R.; Biswas, P.; Saharan, V. Engineered chitosan based nanomaterials: Bioactivities, mechanisms and perspectives in plant protection and growth. *Int. J. Biol. Macromol.* **2018**, *113*, 494–506. [CrossRef] [PubMed]
8. Verlee, A.; Mincke, S.; Stevens, C.V. Recent developments in antibacterial and antifungal chitosan and its derivatives. *Carbohydr. Polym.* **2017**, *164*, 268–283. [CrossRef] [PubMed]
9. Rahman, M.H.; Hjeljord, L.G.; Aam, B.B.; Sørlie, M.; Tronsmo, A. Antifungal effect of chito-oligosaccharides with different degrees of polymerization. *Eur. J. Plant Pathol.* **2015**, *141*, 147–158. [CrossRef]
10. Younes, I.; Sellimi, S.; Rinaudo, M.; Jellouli, K.; Nasri, M. Influence of acetylation degree and molecular weight of homogeneous chitosans on antibacterial and antifungal activities. *Int. J. Food Microbiol.* **2014**, *185*, 57–63. [CrossRef] [PubMed]
11. Kananont, N.; Pichyangkura, R.; Chanprame, S.; Chadchawan, S.; Limpanavech, P. Chitosan specificity for the in vitro seed germination of two *Dendrobium* orchids (Asparagales: Orchidaceae). *Sci. Hortic.* **2010**, *124*, 239–247. [CrossRef]
12. Mohammadi, R.; Eidi, E.; Ghavami, M.; Kassaee, M.Z. Chitosan synergistically enhanced by successive Fe_3O_4 and silver nanoparticles as a novel green catalyst in one-pot, three-component synthesis of tetrahydrobenzo[α]xanthene-11-ones. *J. Mol. Catal. A Chem.* **2014**, *393*, 309–316. [CrossRef]
13. Shukla, S.K.; Mishra, A.K.; Arotiba, O.A.; Mamba, B.B. Chitosan-based nanomaterials: A state-of-the-art review. *Int. J. Biol. Macromol.* **2013**, *59*, 46–58. [CrossRef] [PubMed]
14. Xue, C.; Wilson, L.D. Kinetic study on urea uptake with chitosan based sorbent materials. *Carbohydr. Polym.* **2016**, *135*, 180–186. [CrossRef] [PubMed]
15. Fabra, M.J.; Flores-López, M.L.; Cerqueira, M.A.; de Rodriguez, D.J.; Lagaron, J.M.; Vicente, A.A. Layer-by-Layer Technique to Developing Functional Nanolaminate Films with Antifungal Activity. *Food Bioprocess Technol.* **2016**, *9*, 471–480. [CrossRef]
16. Fortunati, E.; Giovanale, G.; Luzi, F.; Mazzaglia, A.; Kenny, J.; Torre, L.; Balestra, G. Effective Postharvest Preservation of Kiwifruit and Romaine Lettuce with a Chitosan Hydrochloride Coating. *Coatings* **2017**, *7*, 196. [CrossRef]
17. Escamilla-García, M.; Rodríguez-Hernández, M.; Hernández-Hernández, H.; Delgado-Sánchez, L.; García-Almendárez, B.; Amaro-Reyes, A.; Regalado-González, C. Effect of an Edible Coating Based on Chitosan and Oxidized Starch on Shelf Life of *Carica papaya* L., and Its Physicochemical and Antimicrobial Properties. *Coatings* **2018**, *8*, 318. [CrossRef]
18. Siripatrawan, U.; Vitchayakitti, W. Improving functional properties of chitosan films to be used as active food packaging by incorporation with propolis. *Food Hydrocoll.* **2016**, *61*, 695–702. [CrossRef]
19. Torlak, E.; Sert, D. Antibacterial effectiveness of chitosan-propolis coated polypropylene films against foodborne pathogens. *Int. J. Biol. Macromol.* **2013**, *60*, 52–55. [CrossRef] [PubMed]
20. Silva-Castro, I.; Barreto, R.W.; Rodríguez, M.C.H.; Matei, P.M.; Martín-Gil, J. Control of Coffee Leaf Rust by chitosan oligomers and propolis. *Agric. Life Life Agric. Conf. Proc.* **2018**, *1*, 311–315. [CrossRef]
21. Venkatesham, M.; Ayodhya, D.; Madhusudhan, A.; Veera Babu, N.; Veerabhadram, G. A novel green one-step synthesis of silver nanoparticles using chitosan: Catalytic activity and antimicrobial studies. *Appl. Nanosci.* **2012**, *4*, 113–119. [CrossRef]
22. Wang, L.-S.; Wang, C.-Y.; Yang, C.-H.; Hsieh, C.-L.; Chen, S.-Y.; Shen, C.-Y.; Wang, J.-J.; Huang, K.-S. Synthesis and anti-fungal effect of silver nanoparticles-chitosan composite particles. *Int. J. Nanomed.* **2015**, *244*, 2685. [CrossRef]
23. El-Gamal, R.; Nikolaivits, E.; Zervakis, G.I.; Abdel-maksoud, G. The use of chitosan in protecting wooden artifacts from damage by mold fungi. *Electron. J. Biotechnol.* **2016**, *24*, 70–78. [CrossRef]
24. Alfredsen, G.; Eikenes, M.; Militz, H.; Solheim, H. Screening of chitosan against wood-deteriorating fungi. *Scand. J. For. Res.* **2004**, *19*, 4–13. [CrossRef]
25. Ding, X.; Richter, D.L.; Matuana, L.M.; Heiden, P.A. Efficient one-pot synthesis and loading of self-assembled amphiphilic chitosan nanoparticles for low-leaching wood preservation. *Carbohydr. Polym.* **2011**, *86*, 58–64. [CrossRef]

26. Torr, K.M.; Chittenden, C.; Franich, R.A.; Kreber, B. Advances in understanding bioactivity of chitosan and chitosan oligomers against selected wood-inhabiting fungi. *Holzforschung* **2005**, *59*, 559–567. [CrossRef]
27. Nowrouzi, Z.; Mohebby, B.; Younesi, H. Influences of nano-chitosan treatment on physical, mechanical properties and bio resistance of wood. *J. Indian Acad. Wood Sci.* **2014**, *11*, 174–181. [CrossRef]
28. Hussain, I.; Singh, T.; Chittenden, C. Preparation of chitosan oligomers and characterization: Their antifungal activities and decay resistance. *Holzforschung* **2012**, *66*, 119–125. [CrossRef]
29. Eikenes, M.; Alfredsen, G.; Erik, B. Comparison of chitosans with different molecular weights as possible wood preservatives. *J. Wood Sci.* **2005**, *51*, 387–394. [CrossRef]
30. Todaro, L.; Russo, D.; Cetera, P.; Milella, L. Effects of thermo-vacuum treatment on secondary metabolite content and antioxidant activity of poplar (Populus nigra L.) wood extracts. *Ind. Crops Prod.* **2017**, *109*, 384–390. [CrossRef]
31. Karimi, A.; Taghiyari, H.R.; Fattahi, A.; Karimi, S.; Ebrahimi, G.; Tarmian, A. Effects of wollastonite nanofibers on biological durability of poplar wood (*Populus nigra*) against *Trametes versicolor*. *BioResources* **2013**, *8*, 4134–4141. [CrossRef]
32. Spavento, E.M. Caracterización y mejora tecnológica de la madera de *Populus x euramericana* I-214 (Dode) Guinier, austral y boreal, con fines estructurales. Ph.D. Thesis, University of Valladolid, Valladolid, Spain, 2015.
33. *EN 350 Durability of Wood and Wood-Based Products—Testing and Classification of the Durability to Biological Agents of Wood and Wood-Based Materials*; European Committee for Standardization: Bruxelles, Belgium, 2016.
34. Xing, J.-Q.; Ikuo, M.; Wakako, O. Natural resistance of two plantation woods *Populus* × *canadensis* cv. and *Cunninghamia lanceolata* to decay fungi and termites. *For. Stud. China* **2005**, *7*, 36–39. [CrossRef]
35. Diaz, B.; Murace, M.; Peri, P.; Keil, G.; Luna, L.; Otaño, M.Y. Natural and preservative-treated durability of *Populus nigra* cv *Italica* timber grown in Santa Cruz Province, Argentina. *Int. Biodeterior. Biodegrad.* **2003**, *52*, 43–47. [CrossRef]
36. Colom, X.; Carrillo, F.; Nogués, F.; Garriga, P. Structural analysis of photodegraded wood by means of FTIR spectroscopy. *Polym. Degrad. Stab.* **2003**, *80*, 543–549. [CrossRef]
37. Pandey, K.K.; Pitman, A.J. FTIR studies of the changes in wood chemistry following decay by brown-rot and white-rot fungi. *Int. Biodeterior. Biodegrad.* **2003**, *52*, 151–160. [CrossRef]
38. Mohebby, B. Attenuated total reflection infrared spectroscopy of white-rot decayed beech wood. *Int. Biodeterior. Biodegrad.* **2005**, *55*, 247–251. [CrossRef]
39. Sun, T.; Zhou, D.; Xie, J.; Mao, F. Preparation of chitosan oligomers and their antioxidant activity. *Eur. Food Res. Technol.* **2007**, *225*, 451–456. [CrossRef]
40. Silva-Castro, I.; Martín-García, J.; Diez, J.J.; Flores-Pacheco, J.A.; Martín-Gil, J.; Martín-Ramos, P. Potential control of forest diseases by solutions of chitosan oligomers, propolis and nanosilver. *Eur. J. Plant Pathol.* **2017**, *150*, 401–411. [CrossRef]
41. Matei, P.M.; Martín-Ramos, P.; Sánchez-Báscones, M.; Hernández-Navarro, S.; Correa-Guimaraes, A.; Navas-Gracia, L.M.; Rufino, C.A.; Ramos-Sánchez, M.C.; Martín-Gil, J. Synthesis of chitosan oligomers/propolis/silver nanoparticles composite systems and study of their activity against *Diplodia seriata*. *Int. J. Polym. Sci.* **2015**, *2015*. [CrossRef]
42. Martín-Gil, J.; Sánchez-Báscones, M.; Hernández-Navarro, S.; Pérez-Lebeña, E.; Martín-Ramos, P.; Araújo-Rufino, C.; Matei, P.M.; Silva-Castro, I. Composite with anti-microbial activity, comprising two self-assembled components of natural origing, and optianally a component (c) of nanometric size. Patent WO 2016066876A1, 6 May 2016.
43. Larnøy, E.; Eikenes, M.; Militz, H. Evaluation of factors that have an influence on the fixation of chitosan in wood. *Wood Mater. Sci. Eng.* **2006**, *1*, 135–148. [CrossRef]
44. *EN 113 Wood Preservatives—Test Methods for Determining the Protective Effectiveness against Wood Destroying Basidiomycetes—Determination of the Toxic Values*; European Committee for Standardization: Bruxelles, Belgium, 1996.
45. Stössel, P.; Leuba, L.J. Effect of chitosan, chitin and some aminosugar on growth of various soil born phytopathogenic fungi. *J. Phytopathol.* **1984**, *111*, 82–90. [CrossRef]
46. Rabea, E.I.; Badawy, M.E.T.; Stevens, C.V.; Smagghe, G.; Steurbaut, W. Chitosan as antimicrobial agent: Applications and mode of action. *Biomacromolecules* **2003**, *4*, 1457–1465. [CrossRef] [PubMed]

47. Singh, T.; Vesentini, D.; Singh, A.P.; Daniel, G. Effect of chitosan on physiological, morphological, and ultrastructural characteristics of wood-degrading fungi. *Int. Biodeterior. Biodegrad.* **2008**, *62*, 116–124. [CrossRef]
48. Chatterjee, S.; Chatterjee, B.P.; Guha, A.K. A study on antifungal activity of water-soluble chitosan against *Macrophomina phaseolina*. *Int. J. Biol. Macromol.* **2014**, *67*, 452–457. [CrossRef] [PubMed]
49. Marcucci, M.C. Propolis: Chemical composition, biological properties and therapeutic activity. *Apidologie* **1994**, *26*, 83–99. [CrossRef]
50. Zabaiou, N.; Fouache, A.; Trousson, A.; Baron, S.; Zellagui, A.; Lahouel, M.; Lobaccaro, J.M.A. Biological properties of propolis extracts: Something new from an ancient product. *Chem. Phys. Lipids* **2017**, *207*, 214–222. [CrossRef] [PubMed]
51. Oryan, A.; Alemzadeh, E.; Moshiri, A. Potential role of propolis in wound healing: Biological properties and therapeutic activities. *Biomed. Pharmacother.* **2018**, *98*, 469–483. [CrossRef] [PubMed]
52. Pastor, C.; Sánchez-gonzález, L.; Cháfer, M.; Chiralt, A.; González-martínez, C. Physical and antifungal properties of hydroxypropylmethylcellulose based films containing propolis as affected by moisture content. *Carbohydr. Polym.* **2010**, *82*, 1174–1183. [CrossRef]
53. Ali, A.; Chow, W.L.; Zahid, N.; Ong, M.K. Efficacy of propolis and cinnamon oil coating in controlling post-harvest anthracnose and quality of chilli (*Capsicum annuum* L.) during cold storage. *Food Bioprocess Technol.* **2013**, *7*, 2742–2748. [CrossRef]
54. Zhang, Z.; Yang, T.; Mi, N.; Wang, Y.; Li, G.; Wang, L.; Xie, Y. Antifungal activity of monoterpenes against wood white-rot fungi. *Int. Biodeterior. Biodegrad.* **2016**, *106*, 2014–2017. [CrossRef]
55. Gu, C.; Zhang, H.; Lang, M. Preparation of mono-dispersed silver nanoparticles assisted by chitosan-g-poly(E-caprolactone) micelles and their antimicrobial application. *Appl. Surf. Sci.* **2014**, *301*, 273–279. [CrossRef]
56. Kim, S.W.; Jung, J.H.; Lamsal, K.; Kim, Y.S.; Min, J.S.; Lee, Y.S. Antifungal effects of silver nanoparticles (AgNPs) against various plant pathogenic fungi. *Mycobiology* **2018**, *8093*, 53–58. [CrossRef] [PubMed]
57. Narayanan, K.B.; Park, H.H. Antifungal activity of silver nanoparticles synthesized using turnip leaf extract (*Brassica rapa* L.) against wood rotting pathogens. *Eur. J. Plant Pathol.* **2014**, *140*, 185–192. [CrossRef]
58. Mascheroni, E.; Figoli, A.; Musatti, A.; Limbo, S.; Drioli, E.; Suevo, R.; Talarico, S.; Rollini, M. An alternative encapsulation approach for production of active chitosan-propolis beads. *Int. J. Food Sci. Technol.* **2014**, *49*, 1401–1407. [CrossRef]
59. Kaur, P.; Thakur, R.; Choudhary, A. An in vitro study of the antifungal activity of silver/chitosan nanoformulations against important seed borne pathogens. *Int. J. Sci. Technol. Res.* **2012**, *1*, 83–86.
60. Velmurugan, N.; Kumar, G.G.; Han, S.S.; Nahm, K.S.; Lee, Y.S. Synthesis and characterization of potential fungicidal silver nano-sized particles and chitosan membrane containing silver particles. *Iran. Polym. J.* **2009**, *18*, 383–392.
61. Araujo-Rufino, C.; Fernandes-Vieira, J.; Martín-Ramos, P.; Silva-Castro, I.; Fernandes-Côrrea, M.; Matei Petruta, M.; Sánchez-Báscones, M.; Carmen, R.-S.M.; Martín-Gil, J. Synthesis of chitosan oligomers composite systems and study of their activity against *Bipolaris oryzae*. *J. Mater. Sci. Eng. Adv. Technol.* **2016**, *13*, 29–52.
62. He, P.; Davis, S.S.; Illum, L. In vitro evaluation of the mucoadhesive properties of chitosan microspheres. *Int. J. Pharm.* **1998**, *166*, 75–88. [CrossRef]
63. Kofuji, K.; Qian, C.J.; Nishimura, M.; Sugiyama, I.; Murata, Y.; Kawashima, S. Relationship between physicochemical characteristics and functional properties of chitosan. *Eur. Polym. J.* **2005**, *41*, 2784–2791. [CrossRef]
64. Flores-López, M.L.; Cerqueira, M.A.; de Rodríguez, D.J.; Vicente, A.A. Perspectives on Utilization of Edible Coatings and Nano-laminate Coatings for Extension of Postharvest Storage of Fruits and Vegetables. *Food Eng. Rev.* **2016**, *8*, 292–305. [CrossRef]
65. Wang, Y.; Wohlert, J.; Bergenstråhle-Wohlert, M.; Tu, Y.; Ågren, H. Molecular mechanisms for the adhesion of chitin and chitosan to montmorillonite clay. *RSC Adv.* **2015**, *5*, 54580–54588. [CrossRef]
66. Akhtari, M.; Arefkhani, M. Study of microscopy properties of wood impregnated with nanoparticles during exposed to white-rot fungus. *Agric. Sci. Dev.* **2013**, *2*, 116–119.
67. Marin, L.; Moraru, S.; Popescu, M.C.; Nicolescu, A.; Zgardan, C.; Simionescu, B.C.; Barboiu, M. Out-of-water constitutional self-organization of chitosan-cinnamaldehyde dynagels. *Chem. A Eur. J.* **2014**, *20*, 4814–4821. [CrossRef] [PubMed]

68. Özgenç, Ö.; Durmaz, S.; Hakki, I.; Eksi-kocak, H. Determination of chemical changes in heat-treated wood using ATR-FTIR and FT Raman spectrometry. *Spectrochim. Acta Part A Mol. Biomol. Spectrosc.* **2017**, *171*, 395–400. [CrossRef] [PubMed]
69. Chen, H.; Ferrari, C.; Angiuli, M.; Yao, J.; Raspi, C.; Bramanti, E. Qualitative and quantitative analysis of wood samples by Fourier transform infrared spectroscopy and multivariate analysis. *Carbohydr. Polym.* **2010**, *82*, 772–778. [CrossRef]